Resonant Γ-X-Γ magnetotunneling in GaAs-AlAs-GaAs heterostructures

J. J. Finley
Department of Physics, University of Sheffield, Sheffield S3 7RH, United Kingdom

R. J. Teissier
Laboratoire de Microstructures et Microélectronique, CNRS, 196 Avenue Henri Ravera, 92225

M. S. Skolnick and J. W. Cockburn
Department of Physics, University of Sheffield, Sheffield S3 7RH, United Kingdom

R. Grey, G. Hill, and M. A. Pate
Department of Electronic and Electrical Engineering, University of Sheffield, Sheffield S1 3JD, United Kingdom
(Received 17 May 1996)

We report the observation of resonant magnetotunneling between states of different effective mass derived from zone center (Γ) and zone boundary (X) points of the Brillouin zone in single-barrier GaAs/AlAs/GaAs p-i-n heterostructures. Resonances arise in the conductance-bias characteristics for both Landau level index conserving ($\Delta n=0$) and nonconserving transfer ($\Delta n=0$). For $\Delta n=0$ resonances, structure with a splitting proportional to the difference in the cyclotron frequencies ($\omega_c^{\Gamma}-\omega_c^{X}$) is observed, while for $\Delta n=0$ transitions a smaller splitting corresponding to ω_c^{X} is reflected. Analysis of these features enables the transverse (X_{xy}) effective mass in AlAs to be determined. Clear evidence for $k_{\|}$ conserving and nonconserving transfer in the elastic Γ-X_z transfer process is reported. [S0163-1829(96)50232-8]

Indirect gap tunnel structures have received significant theoretical[1–3] and experimental[3,4] attention during recent years. This interest is primarily stimulated by the opportunity such structures provide for studying transport processes between electronic states derived from different symmetry points of the Brillouin zone and characterized by different periodic cell wave functions and effective masses. In a previous publication[3] we identified the Γ-X and X-Γ transfer mechanisms governing resonant tunneling through quasiconfined X states in AlAs barriers by electrical transport and electroluminescence spectroscopy studies. These results showed that the Γ-X-Γ tunneling current arises from transfer via states derived from both conduction-band minima perpendicular (X_x and X_y) and parallel (X_z) to the growth direction (z). Moreover, inelastic tunneling was shown to predominate for the X_{xy} channel, with transfer via X_z states being principally elastic in nature.

In this paper we study the Γ-X_z transfer process and confirm its identification through application of high magnetic fields (B) parallel to the transport direction (z). This permits us to study resonant magnetotunneling of Γ symmetry electrons via Landau levels (LL's) formed from X_z states in the AlAs layer. Previously, magnetotunneling has been studied for GaAs-Al(Ga)As double[5–8] barrier structures, where the LL states involved are all of Γ symmetry and characterized by a similar effective mass. Such work has demonstrated that Γ-Γ magnetotunneling is predominantly elastic, proceeding generally with the conservation of LL quantum number (n).[8] However, in such work transitions which conserve n ($\Delta n=0$) arising from different initial LL's are indistinguishable since they arise simultaneously as a consequence of the equivalent cyclotron energies of the LL states. By contrast, for Γ-X magnetotunneling, we show that the difference in effective mass between the LL states permits the resolution of transitions arising from different initial LL's, with the clear observation of both $\Delta n=0$ and $\Delta n=0$ transfer. A similar situation occurs in interband tunneling studies of InAs-GaSb structures, although in this case LL's from both of the component layers were not resolved separately.[9]

The sample studied was a single p-i-n GaAs/AlAs/GaAs heterodiode, grown by molecular-beam epitaxy and processed into 200-μm-diameter mesas. It consisted of the following layers: 0.5-μm $n=2\times10^{18}$ cm^{-3} GaAs buffer, 500-Å $n=1\times10^{17}$ cm^{-3} GaAs, 500-Å $n=3\times10^{16}$ cm^{-3} GaAs emitter, 50-Å undoped GaAs spacer, 60-Å undoped AlAs barrier, 50-Å undoped GaAs spacer, 0.5-μm $p=1\times10^{17}$ cm^{-3} GaAs collector and 0.5-mm $p=1.10^{18}$ cm^{-3} GaAs top contact. The low n-doping close to the barrier ensures that under forward bias electron tunneling occurs from two-dimensional (2D) emitter states through the AlAs barrier.

We first describe the nature of the 2D-2D Γ-X_z tunneling processes expected at $B=0$ and then discuss the $B=0$ situation, in both cases stressing the consequences of the Γ-X effective-mass difference.[10,11] Figure 1(a) shows a schematic band diagram under an applied forward bias V. The energy separation at a given bias [$\Delta E_{\Gamma-X}(V)$] between the lowest 2D Γ emitter state and the quasiconfined X states in the AlAs layer will decrease with increasing V. When $\Delta E_{\Gamma-X}$ becomes less than the 2D emitter Fermi energy (E_F) resonant tunneling may begin. Figure 1(b) shows schematically the 2D Γ and X subbands at three representative biases V_1, V_2, and V_3 for $\Delta E_{\Gamma-X}$ in the range $E_F \leqslant \Delta E_{\Gamma-X} \leqslant 0$. At each bias, initial (Γ) and final (X) states in which total energy and transverse wave vector ($k_{\|}$) are conserved are represented by open circles, while filled circles indicate final states satisfy-

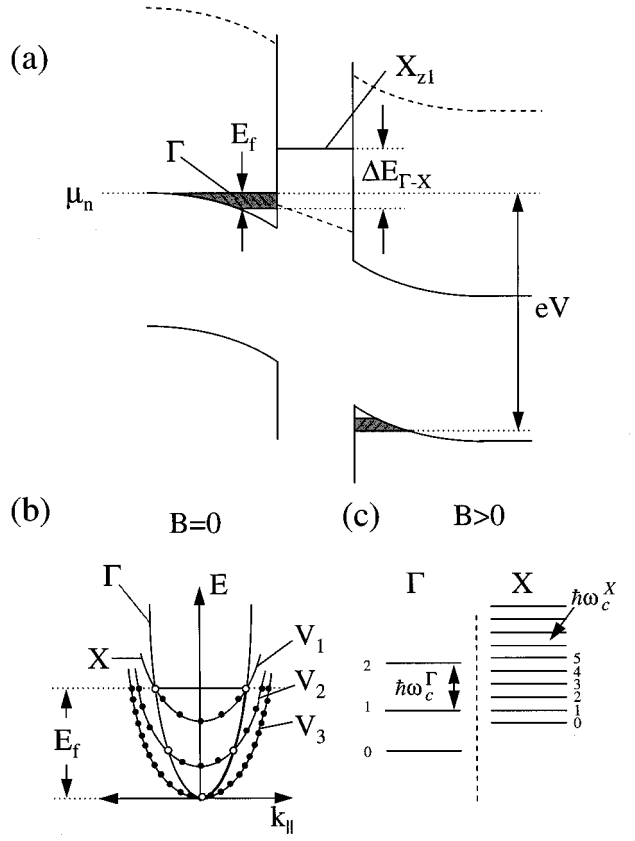

FIG. 1. (a) Schematic diagram of Γ (full line) and *X* (dotted line) band profiles for *p-i-n* GaAs-AlAs-GaAs single barrier heterostructure under applied forward bias. $\Delta E_{\Gamma-X}$ represents the energy separation between the lowest quasiconfined Γ and *X* states. (b) In-plane dispersions of Γ emitter and *X* barrier states at $B=0$. The region below E_f indicates filled emitter states. Open (filled) circles represent *k* states at a given bias to which tunneling can occur with conservation (nonconservation) of in-plane wave vector. (c) Emitter and barrier Landau levels in finite magnetic field.

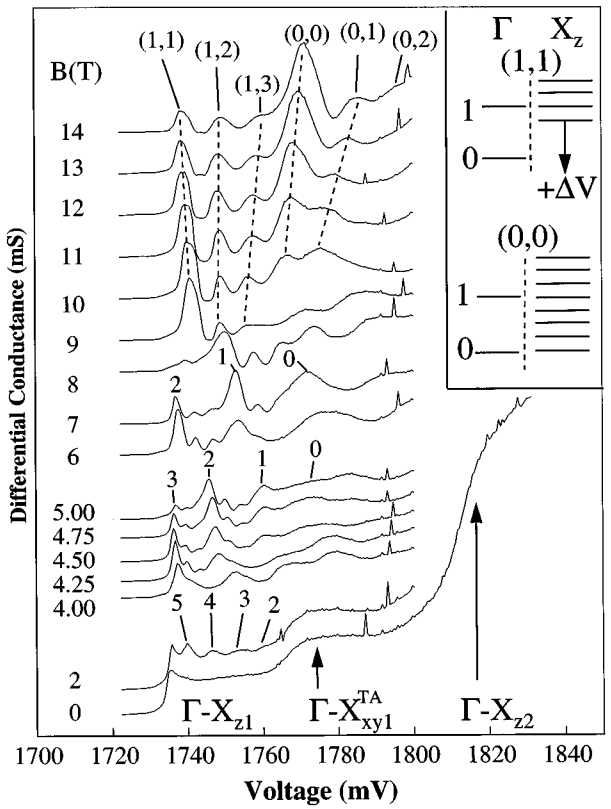

FIG. 2. Conductance-voltage curves at magnetic fields from 0 to 14 T. At $B=0$ $\Gamma\text{-}X_{z1}$, $\Gamma\text{-}X_{xy}^{TA}$, and $\Gamma\text{-}X_{z2}$ features are observed. In finite *B*, the $\Gamma\text{-}X_{z1}$ feature breaks up into well-defined resonances corresponding to (n_Γ, n_X) inter-Landau-level transitions. The inset shows the alignment of the Γ and X_z Landau levels at the (1,1) and (0,0) resonances. For clarity, below 9 T only the n_Γ quantum numbers of the $\Delta n=0$ transitions are labeled.

ing only energy conservation. For *k*-conserving transitions, the Γ-*X* system is resonant over a range of *V* ($V_1<V<V_3$), in contrast to Γ-Γ (2D-2D) tunneling where, in the absence of space-charge buildup, energy and $k_\|$ can only be conserved at a single bias. By contrast for 2D-2D tunneling without $k_\|$ conservation, made allowable by in-plane disorder, resonance will occur over a range of bias for both the Γ-Γ and Γ-X_z cases. Further discussion of the current-voltage (*I-V*) and conductance-voltage (σ_d-*V*) characteristics is given in Ref. 3, where it is also shown that the resonant current is controlled by Γ-*X* transfer, *X*-Γ (collector) tunneling occurring on a much faster time scale due to the greater *X*-Γ wave-function overlap in electric field.

Upon application of magnetic field (*B*), parallel to the growth direction (*z*) the motion in the transverse (*x*,*y*) directions is quantized into LL's with energies $(n+1/2)\hbar\omega_c$, where $n_{\Gamma,X}$ is the LL index in the Γ and *X* subbands, respectively ($n_{\Gamma,X}=0,1,2\ldots$), and ω_c is the cyclotron frequency ($eB/m^*_{\Gamma,X}$). Figure 1(c) shows schematically the relative position of the Γ emitter and *X* barrier LL's at elevated *B*, under a forward bias such that the 1_Γ and 1_X LL's are aligned. Further increase in *V* results in progressively aligning and misaligning the Γ emitter and *X* barrier LL's, with corresponding enhancements in the Γ-*X* transfer rate (and consequently in *I* and σ_d) whenever the condition for LL alignment is satisfied, at biases such that

$$\Delta E_{\Gamma\text{-}X}(B,V)=\hbar eB[(n_x+1/2)/m_X^*-(n_\Gamma+1/2)/m_\Gamma^*] \quad (1)$$

with $m_X^*=m_t^*$ the transverse mass of the X_z valley.[11] Our self-consistent Poisson-Schrödinger[3] calculations show that over the bias range of interest (1730–1800 mV), away from regions of LL depopulation, $\Delta E_{\Gamma-X}$ varies linearly with *V* to better than 8%. As a result, from Eq. (1) resonances are expected in *I-V* with a splitting proportional to $(1/m_\Gamma^*-1/m_X^*)$ for transitions in which $\Delta n=0$ ($n_x=n_\Gamma$). For $\Delta n\neq 0$ ($n_X\neq n_\Gamma$) transfer, analogous to *k*-nonconserving transfer at $B=0$, additional resonances with a periodicity proportional to $1/m_X^*$ are expected arising from each emitter LL.

Figure 2 shows σ_d-*V* data at 1.8 K for *B* ranging from 0 to 14 T, parallel to the tunneling direction. At $B=0$ the data consists of a series of steplike features at 1735, 1765, and 1810 mV. These features arise from elastic and phonon-assisted Γ-*X* transfer between the 2D emitter (Γ) and individual *X* states in the AlAs layer, as identified from self-consistent modeling in Ref. 3. The features at 1735 and 1810 mV were attributed to the thresholds for elastic transfer into X_{zl} and X_{z2} while the step at 1765 mV corresponds to in-

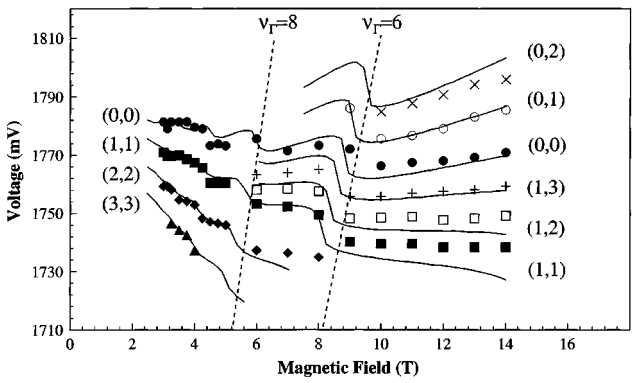

FIG. 3. Plot of resonance biases (the symbols) of Fig. 2 as a function of magnetic field. The full lines are the result of a theoretical simulation of the variation of resonance bias with B, and provide a good fit to experiment. The dashed lines indicate the positions of the bias-dependent integer filling factors for the emitter Landau levels.

elastic transfer into X_{xyl} with the participation of an X point TA phonon. We concentrate below on the Γ-X_{zl} resonance in the bias range 1735–1800 mV, and prove its origin from analysis of the magnetotransport.

For $B>0$ the flat regions in σ_d-V exhibit peaked structure, the amplitude, form, and position of which vary rapidly with increasing B up to ~ 9 T. For $B>9$ T the σ_d-V traces retain their general form, with only the position and amplitude of the features remaining sensitive to further increases in B. To interpret these features, I-B measurements at constant V were performed. The $1/B$ periodicity of the Shubnikov de Haas–like oscillations allows the emitter accumulation density, and hence the electric field in the AlAs to be determined as a function of V,[7] thus permitting the calculation of the bias and magnetic field at which inter-LL resonances are expected. In addition, the LL filling factor in the emitter accumulation layer ($\upsilon_\Gamma=2,4,6\ldots$ including spin) is directly established for a given V and B.

For $V<1800$ mV, at B in excess of 9 T the above measurements indicate that only two emitter LL's are populated (filling favor $\nu_\Gamma<4$), simplifying the identification of the features in Fig. 2. We therefore begin by considering the structure observed for $B>9$ T, where only (n_Γ,n_X) transitions, with $n_\Gamma=0,1$ corresponding to the populated emitter LL's, are expected. A series of peaks labeled $(0,n_x),(1,n_X)$ is observed ($n_x=0,1$, 2, and 3). The peak splitting increases linearly, and the lowest bias peak (1,1) decreases in amplitude as B is increased. At 14 T, the dominant spectral feature, (0,0), is at 1774 mV with weaker peaks to higher bias labeled $(0,n_X)$ ($n_X=1,2$). We identify such structures as arising from resonant (n_Γ,n_X) transfer between the Γ emitter and X_{z1} LL's in the AlAs layer.[12] The $(1,n_X)$ resonances in Fig. 2 weaken with increasing field as the LL degeneracy $(2eB/h)$ increases and the $n_\Gamma=1$ LL depopulates progressively between 9 and 14 T.

The $\Delta n=0$ resonance corresponding to the excited state (1,1) transition is observed at lower applied V than the (0,0) peak. This is a direct consequence of the greater cyclotron energy in the Γ valley.[11] An analogous situation arises for interband resonant tunneling,[9] and is readily understood from Fig. 2 (inset). At the peak of the (1,1) resonance, the

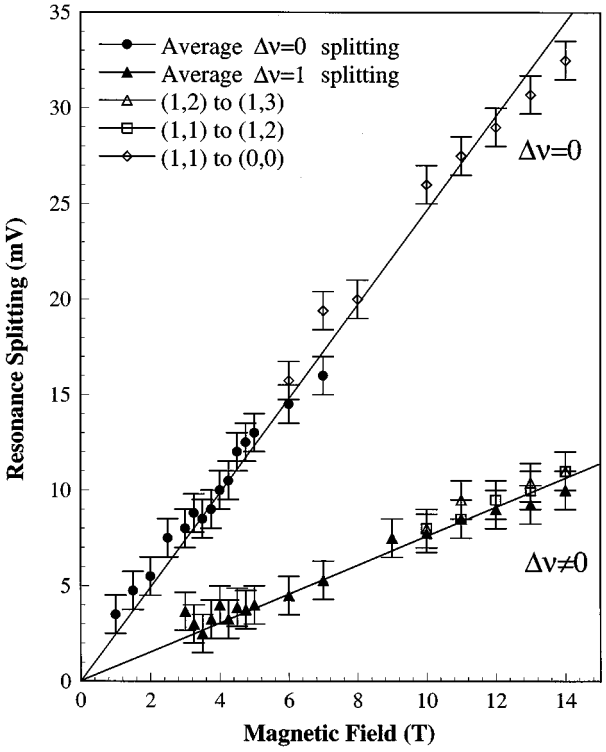

FIG. 4. Voltage splittings of the $\Delta n=0$ and $\Delta n=0$ resonances in Fig. 2 as a function of magnetic field. △, □, and ◇ represent the (1,2)-(1,3), (1,1)-(1,2), and (1,1)-(0,0) splittings, respectively, whereas ▲ and ● are averaged $\Delta\nu=1$ and $\Delta\nu=1$ splittings.

$n_\Gamma=0$ state is $(\hbar\omega_c^\Gamma-\hbar\omega_c^X)$ lower in energy than $n_X=0$ (Fig. 2 inset, *top*). We therefore require a higher bias to reach the (0,0) resonant condition (Fig. 2 inset, *bottom*) with the result that (0,0) is observed at higher V. In addition, between the (1,1) to the (0,0) resonances both the (1,2) and (1,3) transitions are expected since $m_X^*/m_\Gamma^*\sim 4$,[11] in good agreement with Fig. 2. As B is reduced below 9 T, the increase of ν_Γ results in the appearance of higher-order transitions. For example, over the range $6T<B<8T$ $(6>\nu_\Gamma>4)$, the $n_\Gamma=2$ LL is populated, and resonant structure corresponding to $(2,n_X),(1,n_X)$ and $(0,n_X)$ is observed. For B between 4 and 5 T, $8>\nu_\Gamma>6$, and the highest observed n_Γ transition is (3,3).

In order to confirm these identifications, the positions of the resonances observed in σ_d-V are plotted versus magnetic field in Fig. 3 together with the results of an effective-mass calculation. In our calculation, we self-consistently solve the Poisson and Schrödinger equations within the envelope function approximation[3] at $B=0$ to determine the relative energies of the X_{z1} LL's in the AlAs layer and the emitter Fermi level. We include the effect of the magnetic field in the emitter by utilizing an oscillatory Fermi energy (E_F), assuming that the emitter Fermi level remains aligned with the chemical potential in the n-type constant (μ_n) [Fig. 1(a)]. Good agreement with experiment is obtained for both the splittings and slopes of the resonance positions.[13] The peak positions moving with both positive and negative gradients are reproduced correctly. The gradients of different sign arise due to the effective-mass difference between the states involved and may be readily understood if one considers the derivative of

Eq. (1) with respect to B. We have $[\partial(\Delta E_{\Gamma-X})/\partial B] \propto [(n_X+1/2)/m_X^*-(n_\Gamma+1/2)/m_\Gamma^*]$ for transfer from Γ into X_z LL's. As n_X increases, the sign of the gradient may be inverted as the first term of this expression becomes dominant. At the fields corresponding to the bias-dependent integer filling factors (the dashed lines on Fig. 3). LL depopulation and potential renormalization occurs, leading to the observed steps in peak position in Fig. 3.

Figure 4 shows the evolution of the splitting between peaks corresponding to $\Delta n=0$ and $\Delta n\neq 0$ resonances, as B is increased from 0–14 T. Such splitting for $\Delta n\neq 0$ transfer is expected to reflect only the X_z cyclotron energy, whilst the $\Delta n=0$ transitions will exhibit a splitting proportional to the difference in cyclotron energies between the Γ and X_z states. If R is the ratio of the slopes of the $\Delta n=0$ and $\Delta n\neq 0$ transitions in Fig. 4 we have $m_{X_{xy}}^*=(1+R)m_\Gamma^*$. As a result we are able to determine the transverse effective mass ($m_t=m_{X_{xy}}^*$) for the X_z valley without the need to directly establish an energy scale, since $m_\Gamma^*(=0.07m_0)$ is known.[14] Such analysis yields a value of $m_t^*=0.28\pm 0.03m_0$, in excellent agreement with previous determinations utilizing cyclotron resonance[15] ($0.25\pm 0.01m_0$) and magnetoresistance[16] ($0.26\pm 0.03m_0$) techniques. In addition, it confirms the assignment from self-consistent modeling[3] of the 1735-mV threshold in σ_d-V to Γ-X_{z1} transfer. All the structure in Fig. 2 is explained well by Γ-X_z transfer. Features due to X_z spin splitting (1.6 meV at 14 T for[17] $g=2.0$) are not resolved, probably since the splitting is less than the inhomogeneous LL width (5 meV at[13] 14 T). Similarly, Γ-X_{xy}^{TA} LL structure is not observed, probably because the X_{xy}^{TA} width is greater than the LL splitting expected for the $\sqrt{m_t m_1}$ cyclotron mass (2.9 meV at 14 T).

In conclusion, we have reported a magnetotransport study of tunneling through an indirect-gap AlAs single-barrier structure. The effects of the Γ-X effective-mass difference on the magneto-tunneling characteristics have been demonstrated, with clear observation of transfer from individual emitter LL's being observed. Both LL index conserving and nonconserving transfer is shown to occur, with the observation of two periodicities corresponding to the Γ and X electronic states. In addition, the results permit the deduction of the X_{xy} transverse effective mass in AlAs.

We acknowledge M. D. Sturge for very useful discussions and careful reading of the manuscript.

[1] H. C. Liu, Appl. Phys. Lett. **51**, 1019 (1987).

[2] E. L. Ivchenko, A. A. Kiselev, Y. Fu, and M. Willander, Phys. Rev. B **50**, 7747 (1994).

[3] R. Teissier, J. J. Finley, M. S. Skolnick, J. W. Cockburn, M. A. Pate, G. Hill, and R. Grey (unpublished).

[4] E. E. Mendez, W. I. Wang, E. Calleja, and C. E. T. Goncalves da Silva, Appl. Phys. Lett. **50**, 1263 (1987).

[5] E. E. Mendez, L. Esaki, and W. I. Wang, Phys. Rev. B **33**, 2893 (1986).

[6] V. J. Goldman, D. C. Tsui, and J. E. Cunningham, Phys. Rev. B **35**, 9387 (1987).

[7] L. Eaves, G. A. Toombs, F. W. Sheard, C. A. Payling, M. L. Leadbeater, E. S. Alves, T. Foster, P. E. Simmonds, M. Henini, O. S. Hughes, J. C. Portal, G. Hill, and M. A. Pate, Appl. Phys. Lett. **52**, 212 (1987).

[8] M. L. Leadbeater, E. S. Alves, L. Eaves, M. Henini, O. H. Hughes, A. Celeste, J. C. Portal, G. Hill, and M. A. Pate, Phys. Rev. B **39**, 3438 (1989).

[9] E. E. Mendez, H. Ohno, L. Esaki, and W. I. Wang, Phys. Rev. B **43**, 5196 (1991).

[10] H. Ohno and E. E. Mendez, in Appl. Phys. Lett. **56**, 1793 (1990), discuss the consequences of the effective-mass difference for 3D-2D Γ-X tunneling.

[11] The ellipsoidal constant energy surface of the X_z valley is characterized by a longitudinal mass parallel to the tunneling direction of m_1^* of $1.1m_0$, and a transverse mass of m_t^* of $0.28m_0$ determined in the present studies. $m_\Gamma^*=0.067m_0$ the band-edge mass in GaAs.

[12] Elastic transfer into X_{xy} states contributes an unresolved background in this range.

[13] The parameters used in the calculation are a Γ-X band-edge offset of 120 meV from Ref. 3, and the masses given in Ref. 11. The Landau level density of states (DOS) is taken to have the same form as employed by T. P. Smith, W. I. Wang, F. F. Fang, and L. L. Chang, Phys. Rev. B **35**, 9349 (1987) with Gaussian width varying as $1.4B^{0.5}$ meV, and a constant background of 5% of the $B=0$ DOS. Charge accumulation in the barrier is assumed to be negligible at the small current densities employed ($J=4.9\times 10^4$ $A\,m^{-2}$ at $V=1.75$ V). Using an X-Γ scattering time of ~ 1 ps taken from J. Feldman, J. Nunnenkamp, G. Peter, and E. Göbel, Phys. Rev. B **42**, 5809 (1990), a charge density in the AlAs layer of $n_s^{\mathrm{AlAs}}\sim 3.1\times 10^7$ cm^{-2} is deduced, negligible in comparison with the measured emitter accumulation density of $n_s=7.2\times 10^{11}$ cm^{-2} at 1.75 V.

[14] R. Teissier, J. J. Finley, M. S. Skolnick, J. W. Cockburn, R. Grey, G. Hill, and M. A. Pate, Phys. Rev. B **51**, 5562 (1995).

[15] N. Miura, H. Yokoi, J. Kono, and S. Sakaki, Solid State Commun. **79**, 1039 (1991).

[16] S. Yamada, K. Maezawa, T. Yuen, and R. A. Stradling, Phys. Rev. B **49**, 2189 (1994).

[17] H. W. Kesteren, E. C. Cosman, P. Dawson, K. J. Moore, and C. T. Foxon, Phys. Rev. B **39**, 13 426 (1989).